COMPARATIVE AND MATHEMATICAL ANALYSIS OF THE SWIMMING PATTERNS FOR *PARAMECIUM TETRAURELIA*

An Undergraduate Research Scholars Thesis

by

BENJAMIN OFFEREINS

Submitted to the LAUNCH: Undergraduate Research office at
Texas A&M University
in partial fulfillment of requirements for the designation as an

UNDERGRADUATE RESEARCH SCHOLAR

Approved by
Faculty Research Advisor: Dr. Karl J. Aufderheide

May 2022

Major: Biology

RESEARCH COMPLIANCE CERTIFICATION

Research activities involving the use of human subjects, vertebrate animals, and/or biohazards must be reviewed and approved by the appropriate Texas A&M University regulatory research committee (i.e., IRB, IACUC, IBC) before the activity can commence. This requirement applies to activities conducted at Texas A&M and to activities conducted at non-Texas A&M facilities or institutions. In both cases, students are responsible for working with the relevant Texas A&M research compliance program to ensure and document that all Texas A&M compliance obligations are met before the study begins.

I, Benjamin Offereins, certify that all research compliance requirements related to this Undergraduate Research Scholars thesis have been addressed with my Research Faculty Advisor prior to the collection of any data used in this final thesis submission.

This project did not require approval from the Texas A&M University Research Compliance & Biosafety office.

TABLE OF CONTENTS

ABSTRACT

Comparative and Mathematical Analysis of the Swimming Patterns for *Paramecium tetraurelia*

Benjamin Offereins
Department of Biology
Texas A&M University

Research Faculty Advisor: Dr. Karl J. Aufderheide
Department of Biology
Texas A&M University

Paramecium tetraurelia are single celled protists commonly found in freshwater. Each paramecium cell is covered by 3,000 cilia, organized into about 70 precise longitudinal rows. Rows can be inverted 180 degrees through a surgical technique. Paramecia with normal cortex's swim in tight, left-handed helical patterns. Cells with inversions appear to swim in a wider helix with a shorter wavelength, giving a "twisty" pattern. Previous studies done on the inverted swimming pattern of paramecia focused on *P. tetraurelia* Invert E. These studies produced an equation linking the number of inverted rows to the twistiness of the swimming pattern. I examined whether inversions of different sizes and locations on the cell would confirm the trends established by the equation by studying three new inverts. Invert 1 is still being studied. Invert 3's inversion starts at row 41 and is 5 rows wide, which is significantly different from Invert E's that starts at row 26 and is between 5-19 rows wide. Invert 2's inversion starts at row 60 and is 5 rows wide and split by 1 normal row. Analysis of the swimming patterns appeared to show differences between the swimming patterns of Invert 3 and Invert E. Nevertheless, the general trend predicted by the equation holds true: the greater the number of inverted rows the more

twisty the swimming pattern. My research also indicated that swimming patterns are significantly affected by variables that are more difficult to control, such as nutrition, the paramecium's stage in the cell cycle, and size, which increased the variability in my data. Further documentation of the variables of swimming patterns is clearly needed.

DEDICATION

To my loving parents whose endless support has allowed me to have the opportunity to conduct this research.

ACKNOWLEDGEMENTS

Contributors

I would like to thank my faculty advisor, Dr. Karl Aufderheide for his guidance and support throughout the course of this research. Dr. Aufderheide first introduced me to paramecia as a research field and his passion and excitement for them is contagious. Every stain is now a thrilling experience as I focus the microscope to see if the stain was successful and admire the organization of the cilia in their chaotic environment. His dedication to his lab is inspiring and it has been a privilege to work with him on a daily basis.

I would also like to thank Dr. Scott Crawford for providing his expertise and assistance with the statistical analysis and describing the different statical methods to best access my data.

Finally, I would like to thank my fiancée Addison Michaelian for patiently reviewing this document with me and her continued love and support throughout the course of this research.

Funding Sources

Furthermore, I would like to express my gratitude to Dr. Aufderheide for providing his lab and all the materials necessary to conduct this research.

1. INTRODUCTION

1.1 Background

Paramecium tetraurelia are protists commonly found in freshwater. Paramecia are covered by 3,000 cilia, organized into about 70 longitudinal rows. Rows can be inverted 180˚ through a technique using heteropolar doublets (Beisson & Sonneborn, 1965; Aufderheide, 1999). Cilia of the inverted rows beat backwards compared to the normally oriented cilia (Tamm et al, 1975). The inversions ultimately cause an alteration in the organism's swimming pattern, which can be clearly seen when compared to the wild-type. Wild-type paramecia swim in a tight, left-handed helical pattern. Inversions appear to distort the cell's normal swimming pattern (Tamm et al, 1975). Previous studies done on the inverted swimming pattern of paramecia focused on *P. tetraurelia* line InvE (Invert E). In this study, I examined how inversions of different size and location would affect swimming patterns by using 3 newly created invert lines. First, I established the corticotype of each of these inverts. This documents the circumferential location and size of the inverted rows. Then I analyzed their swimming patterns and determined whether previously developed equations by Crookston (Crookston, 2019), Turlington (Turlington, 2016), and Anton (Anton, 2016) are applicable to these new inverts.

1.2 Literature Review

Paramecia were first popularized as a model organism for the study of genetics by Sonneborn in 1937 when he discovered mating types in *P. aurelia*. Paramecia presented a unique ability to study the role of the cytoplasm in heredity (Beale, 1954). Paramecia can exchange genetic material via conjugation and proliferate asexually. Paramecia conjugate by joining at the oral grove forming a pair of cells. The micronuclei of the conjugants divide by meiosis to form

haploid micronuclei. These haploid micronuclei are then exchanged, a diploid zygote nucleus is assembled, and the conjugated cells separate. Each zygote nucleus then undergoes 2 rounds of mitosis from which 4 daughter nuclei are formed. Two of the mitotic products differentiate to form new micronuclei, while the remaining 2 form new macronuclei.

The phenomenon of inverted ciliary rows was first described by Sonneborn and Beisson (Beisson et al, 1965). Their study found that paramecia can develop cortical alterations and pass on those structural differences without changes for many cell cycles. Cortical inversions are developed from paramecia that became "stuck" together while conjugating, forming doublets in the heteropolar position. Some of the progeny of the heteropolar doublets exhibited a twisty swimming pattern, and rows of inverted cilia. These inverted cilia appeared to be rotated 180˚ and as the kinetodesmal fibers always lie slightly to the right of the kinetosome a wide and narrow space was seen separating the inverted rows.

In 1975, Tamm (Tamm et al, 1975) further explored these cortical inverts. This study established that the twisty swimming pattern was indeed due to inverted cilia beating in the opposite direction of normally oriented cilia. Fixing wild-type and inverted paramecia while they were swimming forwards demonstrated that the cilia had an altered power stroke and that they were causing the change in swimming pattern.

A 1999 study by Aufderheide (Aufderheide et al, 1999) further described the structure of inverted ciliary rows. They found that the whole cortical unit was inverted 180˚ showing special wide and narrow junctures at the boundaries between inverted and normally oriented rows. The asymmetry of the cortical unit was confirmed to be the cause of the visible wide and narrow junctures.

In 2014 Bessellieu researched the phenomenon of invert paramecia seemingly losing their inversions over time (Bessellieu, 2014). He found that after only 5 days a significant number of inverted rows could be lost without hand selection when culturing cells. He found that paramecia could spontaneously lose inverted rows and that cells with fewer inverted rows would proliferate faster. This led to cells with significant inversions being quickly outnumbered in a culture. He also found that cells with more inversions tended to exhibit more twisty swimming patterns.

The Anton brothers in 2016 built on this finding establishing a quantitative connection between the number of inverted rows and the twistiness of the swimming pattern (Anton & Anton 2016). By corticotyping and recording the swimming pattern of paramecium with various numbers of inverted rows the brothers were able to establish a clear mathematical connection. They even developed a formula based on the wavelength, diameter, and velocity of the track of a cell's swimming pattern to predict the number of inverted rows.

Turlington refined this equation later that year, finding that the Anton brothers made a mathematical error. Both Turlington and the Antons took separate random samples for swimming pattern and corticotype analysis. Analysis by Turlington, found that taking a single variable approach based on wavelength was able to predict the number of inversions most accurately.

Finally, in 2019 Crookston and Patel further analyzed both the Antons' and Turlington's equations. They ditched the single variable approach and returned to the triple variable approach as they believed it was able to account better for variances in swimming activity and nutrition when recording swimming patterns. They also switched to a paired approach taking the swimming pattern and corticotype of the same cell. Their mathematical analysis led to a further

refined equation. They concluded that the equation, while broadly inaccurate, pointed to a clear first order relationship between swimming pattern and twistiness. Further, they believed that the inaccuracy of the equation was largely due to uncontrollable variables such as nutrition, age, and size.

1.3 Hypothesis and Objectives

Despite cortical inversions having been long studied, all of the mathematical analysis of swimming patterns has been exclusively done with InvE. Generated in 1980, InvE is characterized by having roughly 28 rows of normally oriented cilia. These are followed by between 1 and 20 inverted rows located on the left-dorsal side of the cells. This broad range in the number of inverted rows is what allowed the Anton brothers to initially develop an equation. While the equation is often not consistently accurate, a clearly proportional relationship can be seen between the number of inverted rows and the twistiness of the swimming pattern.

Recently, Dr. Aufderheide was able to isolate some new heteropolar doublets and closely monitor them for the development of any new inverts. From these heteropolar doublets, Dr. Aufderheide isolated 3 new lines of inverts. I corticotyped each new line. The new inverts were fittingly named inverts 1, 2, and 3. My project focused on invert 3 (I3) and the way its swimming pattern compares to that of InvE. Moreover, I examined whether the equations developed by Crookston, Turlington, and Anton would apply to this invert as well. These new lines have cortical inversions in different locations. This not only allows for analysis of the equation, but also a broader analysis on whether the location of the inversion also affects the swimming pattern of the paramecia. The null hypothesis being tested for was that the equations developed by Crookston, Turlington, and Anton would still apply with similar accuracy to paramecia with

inversions in different locations. I believe that the location of the inversion will affect the swimming pattern of the paramecia.

Understanding the swimming patterns and how different variables affect them will help us understand the cell surface patterning of paramecia. Cell surface patterns can have a significant effect on a cell that include implications for a cell's cytoskeleton (Aufderheide et al, 1980). The cytoskeletal effects lead to morphological differences in cells. A better understanding of cell surface patterns and the variables that affect them will lead to better understanding of the phenotypic expression of cells.

2. METHODS

2.1 Maintaining Cell Lines

Cell cultures were maintained according to the standard techniques used for paramecia outlined by Sonneborn (Sonneborn, 1970). The liquid media used was a baked lettuce powder infusion buffered by 5.25 mM sodium phosphate and reinforced by 5mg/L stigmasterol (Aufderheide 1986). *Klebsiella pneumoniae* (ATCC #27889) was used to inoculate the media as a monoxenic food source (Sonneborn, 1970). Four cell lines were kept: the wild-type (*Paramecium tetraurelia* stock 51s, mating type O), Invert 1, Invert 2, and Invert 3. Daily isolations were performed to select for the most augmented swimming pattern exhibited by the inverts (Beisson, 2010).

2.2 Recording Motility Tracks

To record the swimming pattern of the paramecia, cells were washed twice into Dryl's buffer (Dryl, 1959). The paramecia were then placed in a 1mm deep motility chamber treated with silicone to be hydrophobic, which was filled with Dryl's buffer until it was flush with the top of the chamber. Swimming patterns were taken with a Lumenera Scientific Infinity-2 camera using a low-powered (4x objective) using dark-field microscopy for an exposure of 2 seconds (Turlington, 2016).

2.3 Cell Staining

Cell staining was done using a modified Fernández-Galliano silver staining technique (Fernández–Galiano, 1994). This technique has been refined over the past several years first by Dr. Aufderheide (Aufderheide, 2016) and then by Crookston (Crookston, 2019) for staining small numbers of cells in small volumes. I used the Crookston method modifying it further by

changing the 9 μL of 37% formaldehyde solution to 9.5 μL and focusing more on accurate pipetting while adding the reagents, rather than speed.

2.4 Corticotyping

Corticotyping is the process of counting the rows of a paramecia. Counting was performed using the standard technique counting from the left side of the oral apparatus around to the right side of the oral of the oral apparatus under a 100x oil immersion objective lens (Turlington, 2016). Using this technique, the rows from the oral apparatus to the inversion (rows before inversion), the number of rows inverted, and the total number of rows were counted.

2.5 Mathematical Analysis

Table 2.1: Equations Developed to Predict the Number of Inverted Rows

Predictive Equations	
Crookston	IR = 4.126 + (− 0.06773 * λ) + (0.10688 * Amplitude) + (0.03511 * v)
Turlington	IR = 10.9317 + (− 0.01347 * λ) + (0.020967 * Amplitude) + (-0.0135 * v)
Turlington SV	IR = 17.084 + (− 0.0404 * λ)

Note: Table showing the predictive equations for inverted rows (IR) made by Turlington (2016) and Crookston (2019). Turlington single variable (SV) is the equation Turlington developed only using the wavelength parameter.

Mathematical Analysis was done in Microsoft Excel. First, I applied the formula's developed by Crookston and Turlington to my data. The equations (Table 2.1) use the wavelength, amplitude, and velocity from the motility track to predict the number of inverted rows. By performing individual motility track recordings and corticotypes of each paramecium, I was able to do a paired analysis between the predicted and actual number of inverted rows. Further statistical analysis was done on the predicted values generated by Crookston's formula as

it was the most accurate on average. A standard 2 tailed paired T test was performed to assess the equation further.

3. RESULTS

3.1 Corticotyping

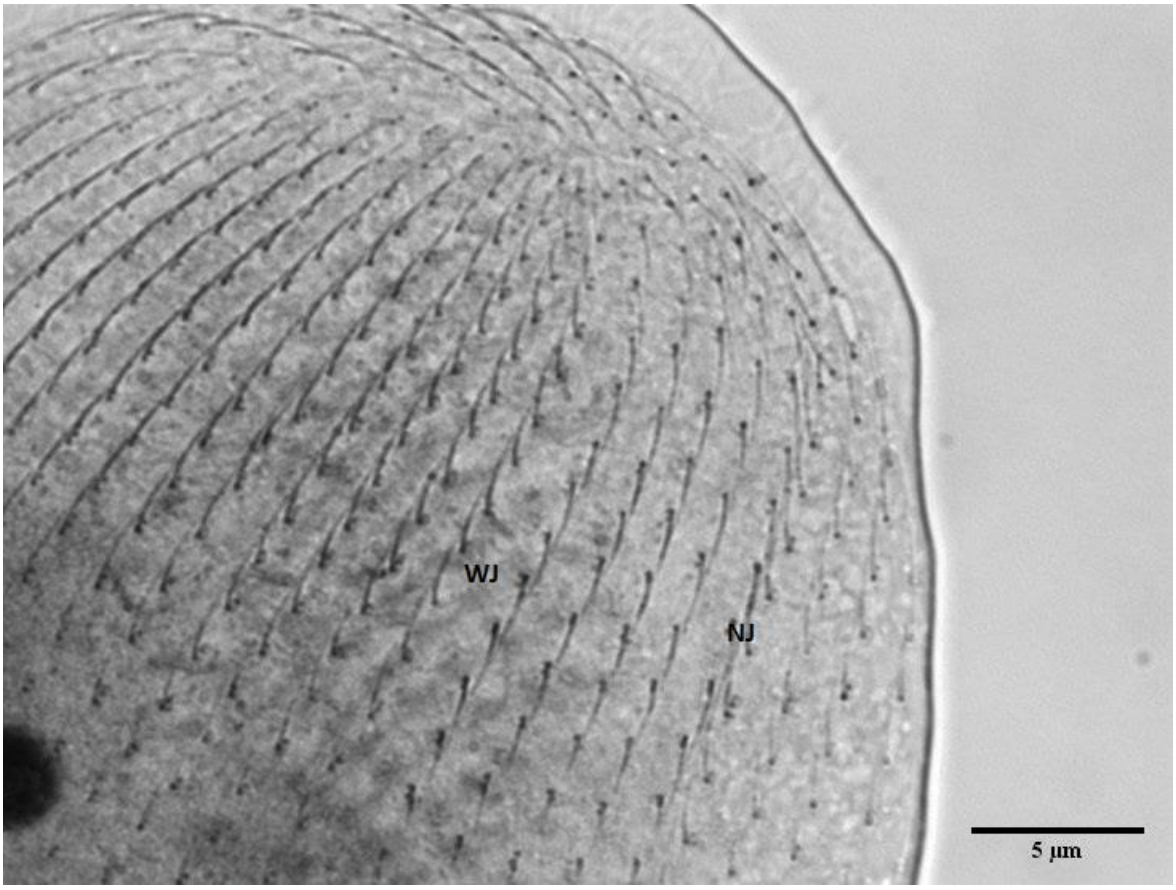

Figure 3.1: I3 stained. Each hair like line is a kinetodesmal fiber. The dark dots at the base of each hair are basal bodies. Clearly depicted near the center of the image are 5 rows of cilia facing the opposite direction. The gap between the inverted and normally oriented cilia on the left is the wide juncture (WJ). The right juncture is the narrow juncture (NJ) where the inverted cilia appear to be touching the normally oriented cilia.

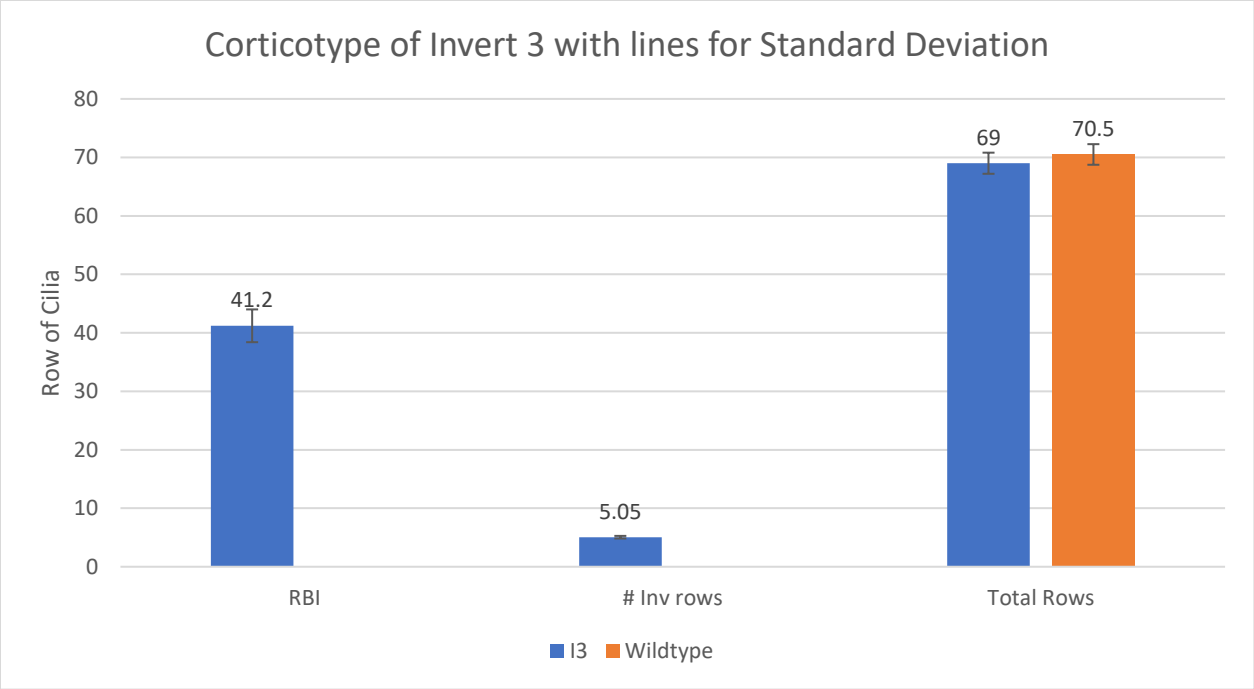

Figure 3.2: A bar graph of the average corticotype of I3 with bars for standard deviation. Rows before the inversion (RBI) is the average number of normal rows before the inversion. Number of inverted rows (# Inv rows) is the average amount of inverted rows. Total rows is the average total count of rows inverted and normal.

I focused my research on the I3 invert line and thus this invert has the most thoroughly examined corticotype (Figure 3.1). Figure 3.2 shows the average corticotype among I3 paramecia. There is little deviation in the data placing the inversion in I3 on the mid-dorsal side of the cell, using the oral apparatus as the marker for the ventral side of the cell. Using the standard corticotyping method of counting from the left side of the oral apparatus, there were on average 41 rows before the inversion. The inversions consistently lasted 5 rows before reverting to normally oriented rows. As expected, the total rows remained near 70 rows with little variation among *Paramecium tetraurelia.* The raw data for the cortiocotyping of InvE and I3 is shown in Table A.1. This varies significantly from InvE, whose inverted rows begin roughly 20 rows in from the left side of the oral apparatus. InvE has often been characterized as having its inversion on the left shoulder. In contrast, I3 could be characterized as having its inversion in the mid-dorsal region sitting slightly to the right.

I also took the Corticotype of invert 2 which started at row 60 and is 5 rows wide and split by 1 normal row. Invert 1 also has a split inversion, but I was unable to take an exact corticotype. Both inverts 1 and 2 need further analysis to establish a complete corticotype.

3.2 Motility Tracks

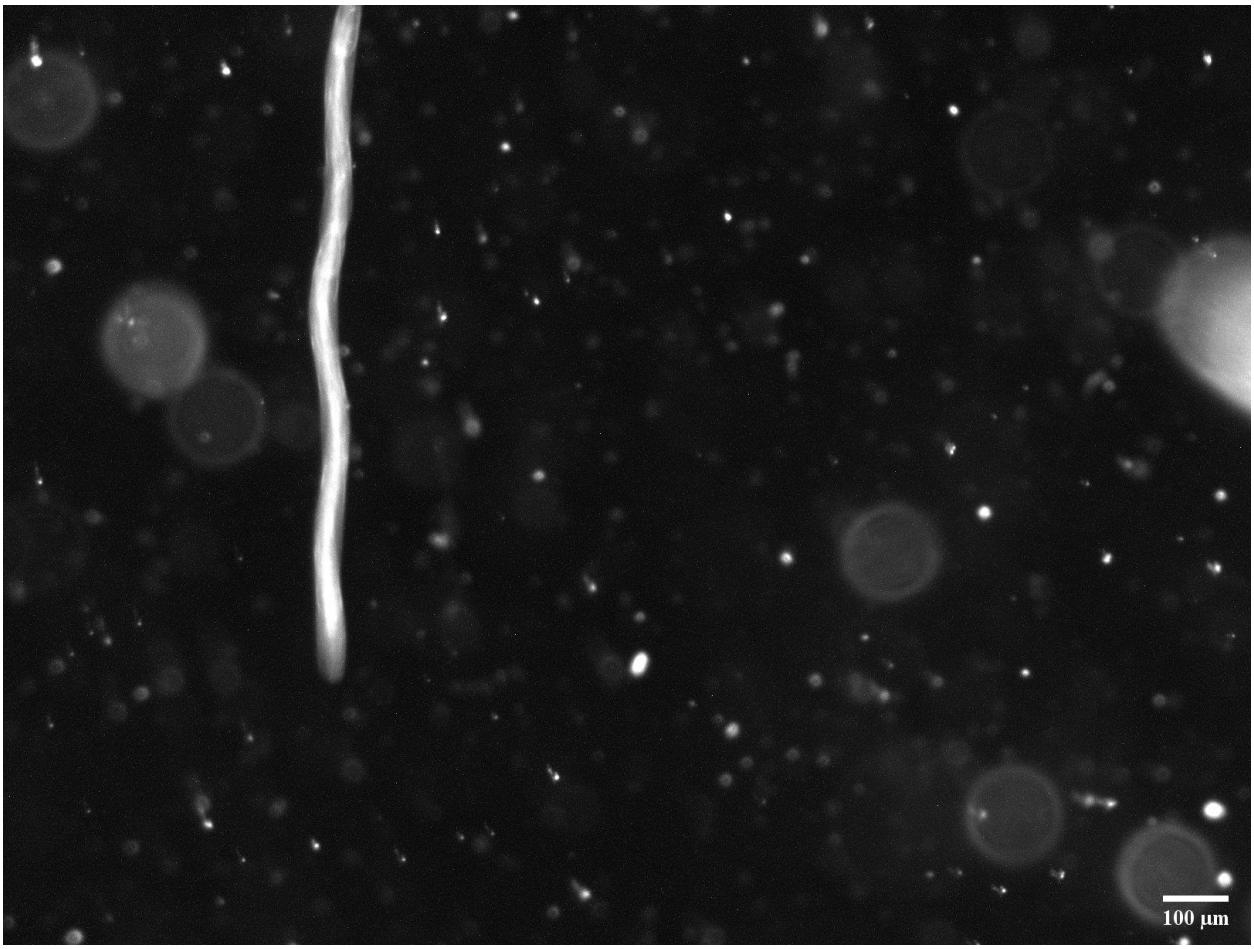

Figure 3.3: Motility track of a wildtype cell in 2 second exposure.

Figure 3.4: Motility track of I3 cell in 2 second exposure.

Paramecia swim in a left-handed helical pattern. Thus, when their motility track is photographed, a wavelike pattern is seen. Measurements were taken from these swimming patterns for wavelength, amplitude, and total length divided by 2 seconds for the velocity of the paramecia. Wavelength and amplitude were easy to record. However, keeping the paramecia in frame for 2 seconds proved challenging. The other random dots scattered across the image are bacteria or microscopic debris. Figure 3.3 depicts a wildtype swimming pattern in which a gentle wave can be seen. Figure 3.4 depicts the swimming pattern of I3. A clear increase in the amplitude of the wave can be seen for the invert. As expected, the wavelength and velocity both decreased slightly, due to the increase in amplitude. This is reflected in the data.

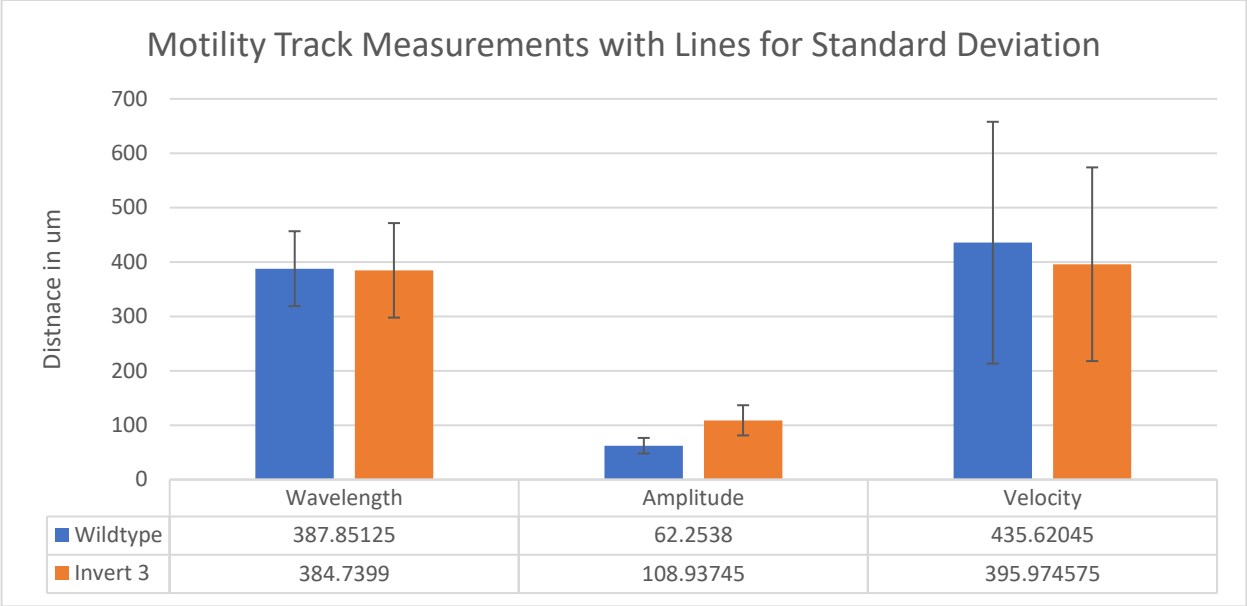

Figure 3.5: A comparison of the motility tracks of I3 and wildtype. All lengths are in µm with bars included for standard deviation. The velocity is in µm/sec.

Figure 3.5 shows the average measurement taken from the motility tracks that are used as parameters in the prediction equation. The wildtype and invert wavelengths are surprisingly similar; however, the amplitude and velocity show clear differences. Motility tracks show a high degree of variability as previously noted by Crookston (Crookston, 2019). The raw data for the motility tracks is shown in Table A.2. Despite the high degree of variability there is a clear pattern of differences between the inverted and wildtype data sets.

Figure 3.6 compares the swimming patterns of I3 and InvE using lines of InvE that also had 5 inverted rows. Antons' and Crookston's data fall within the standard deviation of my data despite the different location of the inversion. While unexpected, this can be attributed to the high degree of variability among motility track data. The similarity points to little difference in swimming patterns despite the different location of the inversion. InvE is unique from I3 in that IE's number of inverted rows is much more variable. This leads to additional variation in the

motility track measurements of Anton and Crookston. Their line of cells had between 3 and 7 inverted rows, while I3 has 5 inverted rows consistently.

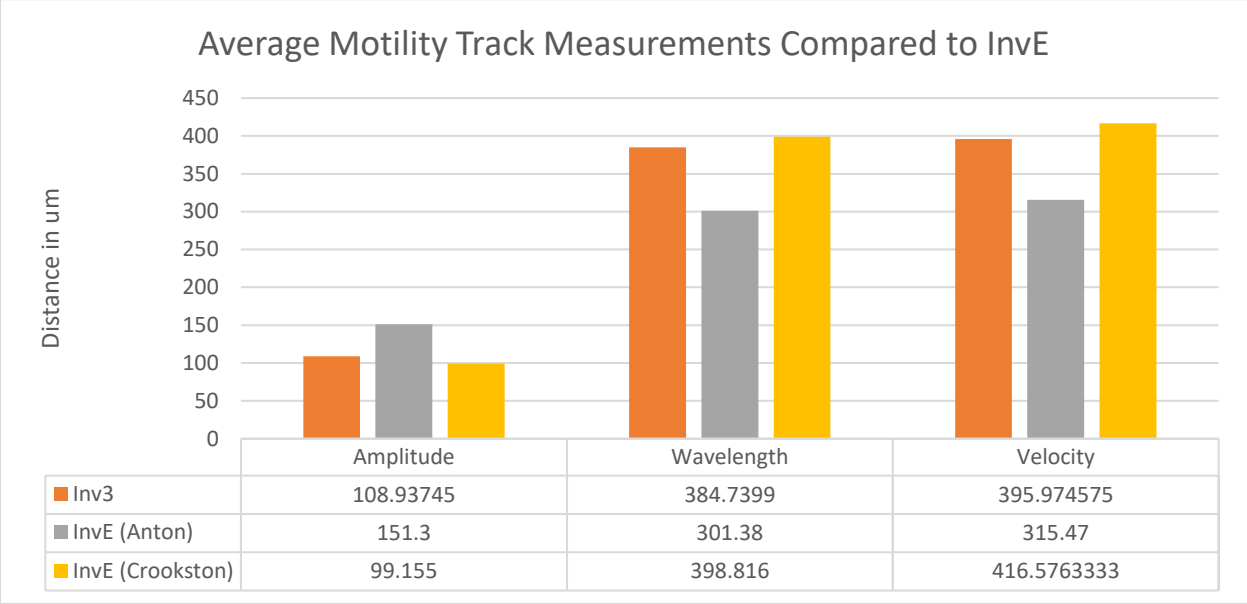

Figure 3.6: Comparison of InvE swimming patterns to I3. All lengths are in µm. The velocity is in µm/sec. I3 is shown in orange. InvE shown in gray is from Anton (Anton, 2016). InvE shown in yellow is from Crookston (Crookston, 2019).

3.3 Mathematical Analysis

Table 3.1: Mathematical Comparison of the Predictive Equations

Testing the Predictive Equation on I3				
Equation	Predicted W	Observed W	Predicted I3	Observed I3
Crookston	-0.19485	0	3.613469	5
Turlington	1.133015	0	2.688934	5
Turlington Single Variable	1.41481	0	1.540508	5

Note: Table showing the average predicted value of wildtype (W) and I3 (I3) compared to the average observed value for the equations in Table 2.1.

Using the predictive equations in Table 2.1, the parameters collected from the motility tracks were used to calculate the predictive number of inverted rows for each equation. Table 3.1

shows the average predicted values compared to observed values for each equation. Due to the significant variance in the swimming track data, there was also high variance in the predictive values from the equations. While Turlington's equations were more consistent than Crookston's, they were also less accurate on average. Looking at the equations, this can be explained by the larger coefficients and smaller constant in Crookston's equation compared to Turlington's.

The above table (Table 3.1) indicates that Crookston's equation was the most accurate. Thus, I performed my statistical analysis using his equation. By performing a paired T test, the accuracy of the predictive equation can be tested for each paramecium. To determine whether the equation was still statistically significant for I3, I performed a paired two tailed T test. Table 3.2 depicts the results of this T test.

Table 3.2: Statistical Comparison of Crookston's Equation Between I3 and InvE

T Test Results		
P-Value	I3	InvE
Wildtype	0.854	----------
Invert	0.189	0.787

Note: Table showing the T test P-values for Crookston's equation. The I3 column are values calculated from my wildtype and I3 data using a paired T test between the observed and predicted values. The InvE column contains the P-value from Crookstons (2019) paper.

The T test provides a prospective of the accuracy of the equation on average. The P-value generated by the T test is a value between 0 and 1 that represents the accuracy of the predictions made by the formula: the higher the P-value, the more accurate the prediction equation. The standard P-value used to reject a predictive hypothesis is $P \leq 0.05$. Thus, in order to reject the predictive equation a P-value of less than 0.05 is necessary. According to the T test I performed, wildtype data fits the equation best. This is surprising, since the equation was modeled after InvE. The equation was designed to include a wildtype prediction of 0 inverted rows, and

Crookston's analysis of the wildtype were less accurate than the predictions for InvE. Still, Crookston's P-Value of 0.787 falls within the expected variable range of 0.854 from the wildtype data I collected. Both P-values are relatively high and provide strong evidence for the accuracy of the equation. However, I3's P-value is significantly lower than the P-value of 0.189 for my wildtype data. While this is not a statistically significant difference, it falls well beyond the expected variation.

4. CONCLUSION

My analysis of the swimming pattern for I3 provides evidence for the general trend predicted by the equation: the greater the number of inverted rows, the more twisty the swimming pattern. However, analysis of the differences between the swimming patterns of I3 and InvE shows some evidence that swimming patterns are affected by the circumferential location of the inversion. Variables that are difficult to control, such as nutrition, the paramecium's stage in the cell division, and the paramecium's size, may have also contributed to variations in the swimming patterns.

From the corticotyping data, I was able to establish a corticotype for I3 of 41 rows before the inversion, followed by 5 inverted rows. This unique corticotype provided the basis for testing the predictive equation on paramecia with inversions in different locations. The corticotype remained consistent with 5 inverted rows. From the corticotyping I did on Inverts 1 and 2 I was able to establish that both had split inversions. Still Inverts 1 and 2 require further analysis to determine a stable corticotype.

Despite the unique inversions, the swimming pattern measurements appeared strikingly similar to those of InvE. All three parameters for InvE—wavelength, amplitude, and velocity—fell well within the standard deviation of my measurements for I3. This provides evidence that the predictive equation would apply well to I3 despite the difference in inversion location. However, the high degree of variability among the measurements was a cause for concern. Many variables were hard to control, and this contributed to the high degree of variability. The size of the paramecium alters the number of total rows. Nutrition and testing time varied depending on the time of day I was able to come into the lab. Another uncontrollable variable was the

paramecium's stage in the cell division cycle. While I attempted to pick paramecia from the culture that were of similar size and similar activity levels, I could not control for these factors. Thus, there was still a significant level of variability among the data. Further research is required to examine the variables' effects on the swimming patterns.

Statistical analysis of the motility tracks showed that despite the apparent similarity in the parameters there was still divergence from the formula's predictions. Crookston's InvE analysis and my wildtype analysis both showed strong evidence for the accuracy of the prediction equation with P-values at roughly 0.8. However, analysis of I3 showed much weaker evidence for the accuracy of the equation with a P-value of only 0.18. To reject the equations, the p-value would have to be statistically significant: less than 0.05. But this difference in p-value is much lower than the expected variance. More data points would be required to achieve statistical significance and establish that the equation does not work for I3.

The similarity in swimming pattern parameters and the high degree of variance provide strong evidence that the lower p-value of I3 is due to the variability in the motility track measurements, and thus, the equation and its general principle hold true. The more inverted rows, the more twisty the swimming pattern. There is also some evidence showing that the location of the inversion might impact the swimming pattern. Further research is needed to demonstrate that the location of the inversion effects the swimming pattern in a statistically significant way.

Ultimately, further analysis of the predictive equation is warranted. Future studies should first focus on the impacts of each of the potential variables affecting the swimming patterns. Finding ways to limit the variables that are difficult to control is vital to being able to establish the full significance of the predictive equation. Feeding the paramecia on a more consistent

schedule and taking the swimming patterns at the same time of day would eliminate some of the variability. Increasing sample size in future studies will help overcome some of the variability when performing the statistical analysis. Pairing the analysis of corticotype and swimming pattern also appeared to provide more accurate results. This is seen in the predictive equation developed by Crookston, which proved to be the most accurate. These further studies on swimming patterns will open a door to a greater understanding of cell movement and cell surface patterns and their importance to the cell.

REFERENCES

Anton, R. M. and Anton, S. M. (2016): Survey Of Swimming Pattern Changes Associated With The Size Of Cortical Inversions In Paramecium tetraurelia. Texas A&M Honors Undergraduate Research Thesis.

Aufderheide, K.J., J. Frankel, and N. Williams (1980): Formation and Positioning of Surface-Related Structures in Protozoa. Microbiological Reviews, June 1980. Vol. 33, No.2 p. 252-302

Aufderheide, K.J. (1986): Identification of the Basal Bodies and Kinetodesmal Fibers in Living Cells of Paramecium tetraurelia Sonneborn, 1975 and Paramecium sonneborni Aufderheide, Daggett & Nerad, 1983. J. Protozool. Vol. 33, No. 1 p. 77-80

Aufderheide, K. J., T. C. Rotolo, and G. W. Grimes. (1999): Analysis of inverted ciliary rows in Paramecium. Combined light and electron microscopic observations. Europ. J. Protistol. 35:81–91.

Aufderheide, K.J. (2016): Refinements of and commentary on the silver staining techniques of Fernández-Galiano. Biotechnic & Histochemistry, 91:5, 352-356, DOI: 10.1080/10520295.2016.1175665

Beale, G. H. (1954): The genetics of Paramecium aurelia. Cambridge University Press, ix.

Beisson, J. and Sonneborn, T.M. (1965): Cytoplasmic inheritance of the organization of the cell cortex in Paramecium aurelia. Proc. Natl. Acad. Sci. 53:275–282.

Beisson, J., Bétermier, M., Bré, M.-H., Cohen, J., Duharcourt, S., Duret, L., Kung, C., Malinsky, S., Meyer, E., Preer, J. R., Jr., and Sperling, L. (2010): Maintaining clonal Paramecium tetraurelia cell lines of controlled age through daily reisolation. Cold Spring Harb. Protoc. DOI: 10.1101/pdb.prot5361.

Bessellieu, J. B. (2014): Structural inheritance and swimming pattern in Paramecium tetraurelia cells with cortical inversions. Texas A&M Honors Undergraduate Research Thesis.

Crookston, C., N. Patel. (2019): Assessment of the Validity of Mathematical Models used to Predict the Number of Inverted Rows on Paramecium tetraurelia. Texas A&M Honors Undergraduate Research Thesis.

Dryl, SJ. (1959): Antigenic transformation in Paramecium aurelia after treatment during autogamy and conjugation. J Protozool 6: S25

Fernández-Galiano, D. (1994): The ammoniacal silver carbonate method as a general procedure in the study of protozoa from sewage (and other) waters. Wat. Res. 28:495–496.

Sonneborn, T. M. (1970): Methods in Paramecium research. Methods Cell Physiol. 4:241–339.

Tamm, S.L., T. M. Sonneborn, and R. V. Dippell. (1975): The role of cortical organization in the control of ciliary beat in Paramecium. J. Cell Biol. 64:98–112

Turlington, K. D. (2016): Assessment of a Predictive Mathematical Formula Relating Swimming Pattern Changes to the Size of Cortical Inversions in Paramecium tetraurelia. Texas A&M University, independent research project.

APPENDIX: RAW DATA

Table A.1: Corticotyping Raw Data for Invert 3 and Wildtype for Control

	Wildtype	RBI	# Inv Rows	Total Rows
1	67	44	5	64
2	71	50	5	72
3	71	42	5	67
4	72	43	5	67
5	73	42	5	69
6	72	43	6	70
7	72	43	5	69
8	68	40	5	69
9	69	42	5	71
10	68	41	5	72
11	71	40	5	69
12	72	38	5	68
13	71	39	5	68
14	72	40	5	70
15	70	40	5	69
16	72	38	5	69
17	69	38	5	68
18	70	41	5	70
19	68	38	5	70
20	72	42	5	69
AVG	70.5	41.2	5.05	69

Note: Table A.1 shows the raw corticotyping data for 20 wildtype and 20 invert 3 paramecia. The first column is the total number of rows for the wildtype paramecia while the following 3 rows are all for the invert 3 paramecia.

Table A.2: Raw Data from Motility Track Measurements

	Wildtype			Invert 3		
	Wavelength	Amplitude	Velocity	Wavelength	Amplitude	Velocity
1	435.156	51.328	475.5825	393.095	131.736	399.8985
2	381.016	58.824	300.1995	353.151	86.472	299.183
3	514.123	76.409	420.1355	462.653	112.86	450.4995
4	330.963	45.939	497.2915	345.492	105	260.4565
5	405.675	51.126	494.659	630.086	138.127	519.03
6	385.104	49.476	682.5475	301.063	93.295	404.7115
7	405.744	55.012	322.8775	401.694	108.997	320.1135
8	232.116	77.294	217.188	437.798	119.042	313.8455
9	365.741	69.757	496.964	397.185	87.745	398.8035
10	380.077	50.046	451.997	422.271	92.601	391.6005
11	371.284	57.016	335.0365	289.619	102.079	338.4595
12	439.513	41.285	464.711	296.341	87.39	364.366
13	341.872	74.986	308.312	326.932	95.448	363.2195
14	351.233	62.824	510.647	376.615	77.713	493.0155
15	445.601	81.913	498.4075	279.511	90.803	274.7315
16	372.218	97.798	321.6995	328.681	135.423	383.3205
17	358.997	67.472	348.0585	428.681	107.515	347.954
18	459.578	54.283	557.896	281.199	89.453	477.0545
19	506.932	69.912	496.229	451.513	115.093	552.6905
20	274.082	52.376	511.97	491.218	201.558	566.538
AVG	387.85125	62.2538	435.6205	384.7399	108.93745	395.9746